Bull. Chem. Soc. Jpn., 73, 2499—2504 (2000)

Structures and Magnetic Properties of Ruthenium(II,III) Pivalate Cation Dimers Axially Coordinated by Pyridyl Nitronyl Nitroxide Radicals through Their Pyridyl Nitrogen Atoms

Yasuyoshi Sayama, Makoto Handa,*,† Masahiro Mikuriya,* Ichiro Hiromitsu,† and Kuninobu Kasuga†

Department of Chemistry, School of Science, Kwansei Gakuin University, Uegahara, Nishinomiya 662-8501

†Department of Material Science, Interdisciplinary Faculty of Science and Engineering, Shimane University, Nishikawatsu, Matsue 690-8504

(Received May 15, 2000)

Adduct complexes of ruthenium(II,III) pivalate dimer with pyridyl nitronyl nitroxide radicals, $[Ru_2(O_2CCMe_3)_4(L)_2]X$ (L = 2-(3-pyridyl)-4,4,5,5-tetramethyl-4,5-dihydro-1*H*-imidazolyl-1-oxyl 3-*N*-oxide (*m*-nitpy) and 2-(4-pyridyl)-4,4,5,5-tetramethyl-4,5-dihydro-1*H*-imidazolyl-1-oxyl 3-*N*-oxide (*p*-nitpy); X = BF_4 and BPh_4), have been prepared and characterized. The dimeric cores, which are axially coordinated by the pyridyl nitrogen atoms of the radical ligands, not by the nitroxide oxygen atoms, have been crystallographically confirmed for complexes with *m*-nitpy (X = BF_4) and *p*-nitpy (X = BPh_4) using an X-ray diffraction method. The magnetic interactions between the radical and Ru(II,III) dimer through the pyridyl group and the radicals of the neighboring cation units through the space are weak.

Nitronyl nitroxide radicals have shown great abilities in combination with paramagnetic transition metal complexes to produce ferro- and ferrimagnetic materials by coordination through their N–O groups.[1] We prepared a nitroxide chain complex of ruthenium(II,III) pivalate cation dimer $[Ru_2(O_2CCMe_3)_4(nitph)]_n(BF_4)_n$, nitph = 2-phenyl-4,4,5,5-tetramethyl-4,5-dihydro-1*H*-imidazol-1-oxyl 3-*N*-oxide, with an expectation for the ferrimagnetic behavior which originates from an alternated arrangement of the radical $S = 1/2$ spin and the ruthenium(II,III) $S = 3/2$ spin. However, the magnetic moment decreased constantly with lowering the temperature, which was accounted for in terms of an unsuitable axial Ru–O–N bond angle for the maganetic interaction.[2] Our efforts to obtain the ferrimagnetic behavior in this combination of Ru(II,III) dimers and nitroxide radicals have all been in vain until now.[3] Pyridyl nitronyl nitroxide radicals have lately been used in combination with transition-metal complexes, and have presented many interesting results by giving an additional magnetic pathway through the pyridyl group.[4] This approach could be applicable to our system. We started research concerning Ru(II,III) carboxylate cation dimers coordinated by the pyridyl groups of the nitroxde radicals. As a part of this work, we reported a ferromagnetic chain complex, $[Ru_2(O_2CCMe_3)_4(p\text{-nitpy})]_n(BF_4)_n$ (*p*-nitpy is defined below), with axial coordinations of one of the two N–O groups and the pyridyl group, in which the spin interaction ($J = 20$ cm^{-1}) through the N–O group is much larger than that ($J' = 0.45$ cm^{-1}) through the pyridyl group.[5] In this study, bis-adduct ruthenium(II,III) complexes, $[Ru_2(O_2CCMe_3)_4(L)_2]X$ (L = 2-(3-pyridyl)-4,4,5,5-tetramethyl-4,5-dihydro-1*H*-imidazolyl-1-oxyl 3-*N*-oxide (*m*-nitpy) and 2-(4-pyridyl)-4,4,5,5-tetramethyl-4,5-dihydro-1*H*-imidazolyl-1-oxyl 3-*N*-oxide (*p*-nitpy); X = BF_4 and BPh_4), were newly prepared and investigated for the magnetic interaction through the coordinated pyridyl group.

Experimental

Preparation of Complexes. The starting materials, $[Ru_2(O_2CCMe_3)_4(H_2O)_2]BF_4$ and $[Ru_2(O_2CCMe_3)_4(H_2O)_2]BPh_4$, were prepared according to a method described in the literature.[6] The axial water molecules of $[Ru_2(O_2CCMe_3)_4(H_2O)_2]BF_4$ were removed before use by heating under a vacuum. The radicals *m*-nitpy and *p*-nitpy were also obtained according to a method described in the literature.[7]

$[Ru_2(O_2CCMe_3)_4(m\text{-nitpy})_2]BF_4$ (1). A 20 mg (0.027 mmol) water-coordinated starting material, $[Ru_2(O_2CCMe_3)_4(H_2O)_2]BF_4$, was employed for a reaction with the radical *m*-nitpy (14 mg, 0.060 mmol) in CH_2Cl_2 (3 cm^3) under argon. Onto the reacted solution of $[Ru_2(O_2CCMe_3)_4(H_2O)_2]BF_4$ and *m*-nitpy was slowly added hexane (15 cm^3); the resulting solution was kept quiet at room temperature for several days. Formed blackish-green crystals were filtered off, washed with hexane, and dried under a vacuum. The yield was 23 mg (73% based on $[Ru_2(O_2CCMe_3)_4(H_2O)_2]BF_4$). Anal. Found C, 45.19; H, 5.94; N, 7.14. Calcd for $C_{44}H_{68}BF_4N_6O_{12}Ru_2$: C, 45.47; H, 5.90; N, 7.23%.

$[Ru_2(O_2CCMe_3)_4(m\text{-nitpy})_2]BPh_4\cdot 0.5CH_2Cl_2$ ($2\cdot 0.5CH_2Cl_2$). The tetraphenyborate salt, $[Ru_2(O_2CCMe_3)_4(H_2O)_2]BPh_4$ (20 mg, 0.021 mmol), and the radical *m*-nitpy (12 mg, 0.051 mmol) were reacted in a 1 : 1 solvent mixture of CH_2Cl_2 (2 cm^3) and hexane (2 cm^3) under argon. Onto the reacted solution was slowly added hexane (15 cm^3); the resulting solution was kept quiet at -1 °C in a refrigerator for several days. Formed blackish-green crystals were fil-

tered off, washed with haxane, and dried under a vacuum. The yield was 23 mg (76% based on $[Ru_2(O_2CCMe_3)_4(H_2O)_2]BPh_4$). Anal. Found C, 57.64; H, 6.26; N, 6.15. Calcd for $C_{68.5}H_{89}BClN_6O_{12}Ru_2$: C, 57.25; H, 6.24; N, 5.85%.

$[Ru_2(O_2CCMe_3)_4(p\text{-nitpy})_2]BF_4$ (3). This compound was obtained as blackish-green crystals by employing 21 mg (0.029 mmol) of $[Ru_2(O_2CCMe_3)_4(H_2O)_2]BF_4$ and 16 mg (0.068 mmol) of *p*-nitpy for a reaction in a similar manner to that of **1**. The yield was 30 mg (89% based on $[Ru_2(O_2CCMe_3)_4(H_2O)_2]BF_4$). Anal. Found C, 45.30; H, 5.96; N, 7.07. Calcd for $C_{44}H_{68}BF_4N_6O_{12}Ru_2$: C, 45.47; H, 5.90; N, 7.23%.

$[Ru_2(O_2CCMe_3)_4(p\text{-nitpy})_2]BPh_4$ (4). This compound was obtained as blackish-green crystals by employing 20 mg (0.021 mmol) of $[Ru_2(O_2CCMe_3)_4(H_2O)_2]BPh_4$ and 16 mg (0.068 mmol) of *p*-nitpy for a reaction in a similar manner to that of **2**·0.5CH_2Cl_2. The yield was 16 mg (55% based on $[Ru_2(O_2CCMe_3)_4(H_2O)_2]$-$BPh_4$). Anal. Found C, 58.36; H, 6.17; N, 5.92. Calcd for $C_{68}H_{88}BN_6O_{12}Ru_2$: C, 58.56; H, 6.36; N, 6.03%.

Measurements. Elemental analyses for carbon, hydrogen, and nitrogen were carried out using a Perkin–Elmer Series II, CHN/O Analyzer. Infrared spectra (KBr pellets) and electronic spectra were measured with JASCO IR-700 and Shimadzu UV-3100 spectrometers, respectively. The magnetic susceptibilities were measured over the 2—300 K temperature range on a Quantum Design MPMS-5S SQUID susceptometer operating at a magnetic field of 0.5 T. The susceptibilities were corrected for diamagnetism of constituent atoms using Pascal's constant.[8] The effective magnetic moments were calculated from the equation $\mu_{eff} = 2.828\sqrt{\chi T}$, where χ is the magnetic susceptibility per Ru(II,III)–(nitroxide)$_2$ unit.

X-Ray Crystal Structure Analysis. Crystals of $[Ru_2(O_2CCMe_3)_4(m\text{-}nitpy)_2]BF_4$ (**1**) and $[Ru_2(O_2CCMe_3)_4(p$-$nitpy)_2]BPh_4$·0.5CH_2Cl_2 (**4**·0.5CH_2Cl_2) were suitable for a single-crystal X-ray structure determination. Diffraction data were collected on an Enraf–Nonius CAD4 diffractometer using graphite-monochromated Mo $K\alpha$ radiation at 25±1 °C. The lattice constants were determined by a least-squares refinement based on 25 reflections with $20 \leq 2\theta \leq 30°$. The intensity data were corrected for Lorentz-polarization effects. The structures were solved by direct methods. Refinements were carried out by the full-matrix least-squares method. The non-hydrogen atoms were refined with anisotropic thermal parameters. The methyl groups of pivalate ions and the solvent CH_2Cl_2 molecule for **4**·0.5CH_2Cl_2 were refined isotropically. There were disorders at carbon atoms of the *t*-butyl groups of **1** and **4**·0.5CH_2Cl_2 and the CH_2Cl_2 molecule of **4**·0.5CH_2Cl_2, and hence their positions were divided with the same or different weights. Hydrogen atoms were fixed at their calculated positions. The weighting scheme, $w = 1/[\sigma^2(|F_o|) + (0.02|F_o|)^2 + 1.0]$, was employed. The final discrepancy factors, $R = \sum||F_o| - |F_c||/\sum|F_o|$ and $R_w = [\sum w(|F_o| - |F_c|)^2/\sum|F_o|^2]^{1/2}$, are listed in Table 1. All of the calculations were carried out on a VAX station 4000 90A computer using a MolEN program package.[9] The relevant bond lengths and angles for **1** and **4**·0.5CH_2Cl_2 are summarized in Table 2. The anisotropic thermal parameters of non-hydrogen atoms and atomic coordinates are deposited as Document No. 73062 at the Office of the Editor of Bull. Chem. Soc. Jpn. Crystallographic data have been deposited at the CCDC, 12 Union Road, Cambridge CB2 1EZ, UK and copies can be obtained on request, free of charge, by quoting the publication citation and deposition numbers CCDC 149030, 149031.

Results and Discussion

The elemental-analytical data demonstrated that the desired bis-adduct complexes, $[Ru_2(O_2CCMe_3)_4(L)_2]X$ (L = *m*-nitpy and *p*-nitpy; X = BF_4 and BPh_4), were formed when more than two-times as much as the nitroxide radicals to the Ru(II,III) salts were employed, though the reaction using an equimolar amount of Ru(II,III) salts and the radicals gave the 1 : 1 complexes presumed to be the chain complex $[Ru_2(O_2CCMe_3)_4(m\text{- or }p\text{-nitpy})]_n(BF_4)_n$.[5] The data

Table 1. Crystal Data and Data Collection Details

	1	**4**·0.5CH_2Cl_2
Formula	$C_{44}H_{68}BF_4N_6O_{12}Ru_2$	$C_{68.5}H_{89}BClN_6O_{12}Ru_2$
F.W.	1162.20	1437.10
Crystal system	triclinic	monoclinic
Space group	$P\bar{1}$	$P2/n$
a/Å	11.305(5)	16.705(3)
b/Å	14.370(6)	13.902(2)
c/Å	9.597(4)	17.707(3)
α/°	103.81(2)	90
β/°	102.99(2)	110.40(1)
γ/°	71.59(4)	90
V/Å^3	1417(1)	3854(1)
Z	1	2
D_c/g cm^{-3}	1.36	1.30
D_m/g cm^{-3}	1.34	1.28
Crystal size/mm	0.60 × 0.39 × 0.35	0.40 × 0.38 × 0.20
μ(Mo $K\alpha$)/cm^{-1}	5.90	4.83
2θ range/°	1.0—50.0	1.0—50.0
No. of reflections measured	4986	7071
No. of unique reflections with $I > 3\sigma(I)$	4340	4155
R	0.026	0.052
R_w	0.033	0.067

Table 2. Relevant Bond Lengths (Å) and Angles (°) with the Estimated Standard Deviations in Parentheses for **1** and **4**·0.5CH_2Cl_2

1[a]		**4**·0.5CH_2Cl_2[b]	
Ru–Ru′	2.276(1)	Ru–Ru′	2.282(1)
Ru–O1	2.018(2)	Ru–O1	2.019(4)
Ru–O2′	2.020(2)	Ru–O2′	2.018(4)
Ru–O3	2.017(3)	Ru–O3	2.009(5)
Ru–O4′	2.015(3)	Ru–O4′	2.007(5)
Ru–N3	2.269(3)	Ru–N3	2.282(6)
O5–N1	1.273(4)	O5–N1	1.27(1)
O6–N2	1.274(4)	O6–N2	1.27(1)
Ru′–Ru–N3	176.5(1)	Ru′–Ru–N3	173.9(2)

a) Primes refer to the equivalent positions (−x, −y, −z). b) Primes refer to the equivalent positions (1 − x, −y, −z).

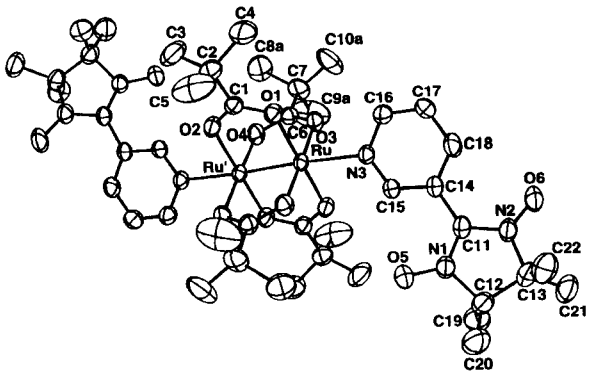

Fig. 1. View of structure of $[Ru_2(O_2CCMe_3)_4(m\text{-nitpy})_2](BF_4)$ (**1**), showing the atom-labeling scheme. Thermal ellipsoids are at the 35% probability level. There are disorders at carbon atoms on a *t*-butyl group, of which those labeled with a are depicted for each of the pairs of the disordered atoms. BF_4^- ions are omitted for clarity. Primes refer to the equivalent positions (−x, −y, −z).

concerning selected IR bands, electronic absorptions in the reflectance spectra, and magnetic moments at 300 K are summarized in Table 3 for the obtained complexes and their parent complexes, $[Ru_2(O_2CCMe_3)_4(H_2O)_2]X$ (X = BF_4 and BPh_4).[10] The stretching carbonyl modes of the parent complexes in the 1500—1400 cm^{-1} region were observed for complexes **1**—**4** in the same region. The predominant bands due to the BF_4^- ion are shown around 1050 cm^{-1} for complexes **1** and **3**.[11] The N–O stretching bands (1368 cm^{-1} for free *m*-nitpy and 1362 cm^{-1} for free *p*-nitpy) can be seen at ca. 1370 cm^{-1} for complexes **1**—**4**. In the diffuse reflectance spectra, the bands observed for the Ru(II,III) cationic dimer (270, 305(sh), 430, 545 (sh), 985(br) nm for the tetrafluoroborate salt; 265, 305(sh), 430, 545(sh), 1000 nm for the tetraphenylborate salt) are all shifted in their positions for the present complexes. These IR and reflectance spectral data support the formation of the desired bis-adduct Ru(II, III) complexes.

X-ray structural analyses were performed for $[Ru_2(O_2CCMe_3)_4(m\text{-nitpy})_2]BF_4$ (**1**) and $[Ru_2(O_2CCMe_3)_4(p\text{-nitpy})_2]BPh_4$·0.5$CH_2Cl_2$ (**4**·0.5CH_2Cl_2). The bis-adduct structure of **1** is depicted in Fig. 1. A crystallographic inversion center is located at the midpoint of the Ru–Ru′ bond of the Ru(II,III) core. The Ru–Ru′ bond distance is 2.276(1) Å, which is in the range of those (2.24—2.30 Å) reported for Ru(II,III) carboxylate dimers.[12] The axial positions of the Ru(II,III) core are occupied by the pyridyl nitrogen atoms of the two nitronyl nitroxide molecules with a separation of 2.269(3) Å. The Ru′–Ru–N3 angle is 176.5(1)°. The two N–O bond lengths (1.273(4) (N1–O5) and 1.274(4) (N2–O6) Å) indicate that the nitronyl nitroxide exists as a free radical.[1b] The dihedral angle between the mean plane formed by O5–N1–C11–N2–O6 and the pyridyl ring is 30.4(2)°. The angle is not unusual compared with those recently reported for the nitroxide adducts of copper(II) carboxylate dimers, $[Cu_2(O_2CCMe_3)_4(p\text{-nitpy})_2]$ (9.47(23)°), $[Cu_2(O_2CMe)_4(p\text{-nitpy})_2]$ (26.08(12)°), $[Cu_2(O_2CCH_2Ph)_4(m\text{-nitpy})_2]$ (28.76 (9)°), and $[Cu_2(O_2CMe)_4(m\text{-nitpy})]_n$ (29.5 (3)°).[4m,4n] The closest contact distances between the nitroxide N–O groups of two *m*-nitpy molecules of neighboring catonic units are as follows: O6···O6″ = 3.981(4) Å and N2···O6″ = 3.836(4) Å (the double primes refer to the equivalent positions (-x, -y-1, -z)). This kind of close contact has been reported for other pyridyl nitroxide complexes.[1b] The bis-adduct cation unit of **4**·0.5CH_2Cl_2 is shown in Fig. 2. The crystallographic

Table 3. Infrared and Electronic Spectral Data and Magnetic Moments at 300 K.

	IR/cm^{-1}			λ_{max}/nm	μ_{eff}/B.M.
	OCO	NO	BF_4^-		(300 K)
1	1482, 1451, 1419	1369	1051	280(sh), 375, 600, 1115(br)	4.72
2·0.5CH_2Cl_2	1483, 1450, 1420	1370		225(sh), 290, 375, 605, 650, 1120(br)	5.04
3	1483, 1453, 1418	1371	1057	275, 360, 450(sh), 585, 640, 1040(br)	4.79
4	1485, 1455, 1421	1373		320, 380, 460(sh), 630, 1030(br)	4.76
$[Ru_2(O_2CCMe_3)_4(H_2O)_2]BF_4$	1486, 1456, 1425		1056	270, 305(sh), 430, 545(sh), 985(br)	4.31
$[Ru_2(O_2CCMe_3)_4(H_2O)_2]BPh_4$	1485, 1448, 1423			265, 305(sh), 430, 545(sh), 1000	4.28

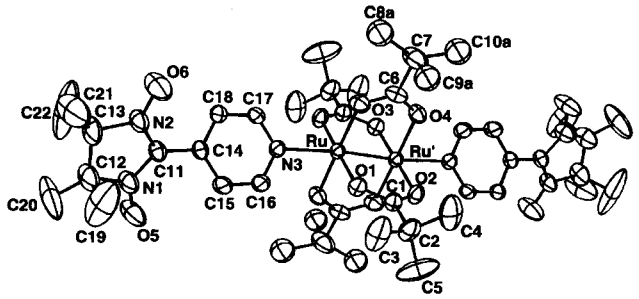

Fig. 2. View of structure of $[Ru_2(O_2CCMe_3)_4(p\text{-nitpy})_2]$-$(BPh_4)\cdot 0.5CH_2Cl_2$ ($\mathbf{4}\cdot 0.5CH_2Cl_2$), showing the atom-labeling scheme. Thermal ellipsoids are at the 35% probability level. There are disorders at carbon atoms on a *t*-butyl group, of which those labeled with a are depicted for each of the pairs of the disordered atoms. BPh_4^- ions are omitted for clarity. Primes refer to the equivalent positions ($1-x$, $-y$, $-z$).

inversion center is located at the midpoint of the Ru–Ru′ bond, of which the distance is 2.282(1) Å. The pyridyl group of *p*-nitpy coordinates to the dimer unit with a distance of 2.282(6) Å. The Ru′–Ru–N3 angle is 173.9(2)°. The N–O bond lengths are 1.27(1) Å (for N1–O5 and N2–O6), indicating that *p*-nitpy exists as a genuine radical.[1b] The dihedral angle between the mean plane formed by O5–N1–C11–N2–O6 and the pyridyl ring is 34.2(8)°, which is comparable to that for **1** and larger than the uncoordinated one (22.8(1)°.[13] The closest distance between the nitroxide oxygen atoms of the neighboring cationic units O5···O5″ is 3.79(1) Å (the double prime refers to the equivalent position ($3/2-x$, y, $1/2-z$)). The contact mode is different from that in **1**, which is schematically shown in Fig. 3.

The effective magnetic moments (per Ru(II,III)–(nitroxide)$_2$ unit) for complexes **1**—**4** at room temperature (4.72—5.04 B.M. (Table 3)) are close to that (4.58 B.M.) expected for noninteracting spins, one $S = 3/2$ (Ru(II,III) core) and

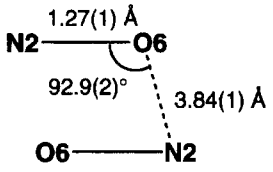

a) $[Ru_2(O_2CCMe_3)_4(m\text{-nitpy})_2]BF_4$ (**1**)

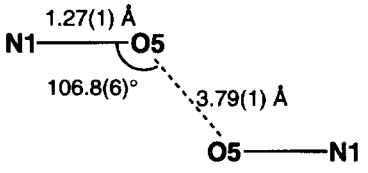

b) $[Ru_2(O_2CCMe_3)_4(p\text{-nitpy})_2]BPh_4\cdot 0.5CH_2Cl_2$ ($\mathbf{4}\cdot 0.5CH_2Cl_2$)

Fig. 3. Contact feature of two NO groups for **1** and $\mathbf{4}\cdot 0.5CH_2Cl_2$.

two $S = 1/2$ (*m*- or *p*-nitpy), which implies that the magnetic interactions between the paramagnetic centers are essentially weak. The temperature dependence of the magnetic moments of **1**—**4** are displayed in Figs. 4—7. All of the complexes show decreases in the moments with lowering the temperature due to the strong zero-field splitting

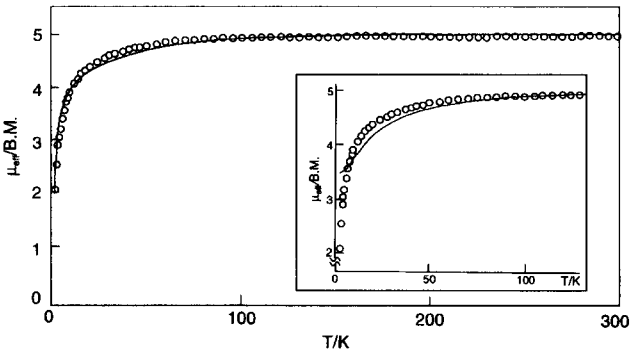

Fig. 4. Temperature dependence of magnetic moment per Ru(II,III)–(*m*-nitpy)$_2$ unit for **1**. The solid line is drawn with parameters listed in Table 4. In the inset, the variable temperature dependence of magnetic moment is simulated based on model B with parameters $g_M = 2.3$, $g_{nit} = 2.0$, $D = 50\ cm^{-1}$, $J_{M-R} = 0\ cm^{-1}$, and $J_{R\cdots R} = -10\ cm^{-1}$.

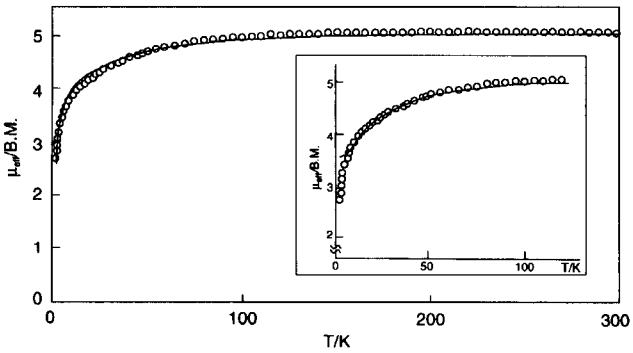

Fig. 5. Temperature dependence of magnetic moment per Ru(II,III)–(*m*-nitpy)$_2$ unit for $\mathbf{2}\cdot 0.5CH_2Cl_2$. The solid line is drawn with parameters listed in Table 4. In the inset, the variable temperature dependence of magnetic moment is simulated based on model B with parameters $g_M = 2.3$, $g_{nit} = 2.0$, $D = 50\ cm^{-1}$, $J_{M-R} = 0\ cm^{-1}$, and $J_{R\cdots R} = -10\ cm^{-1}$.

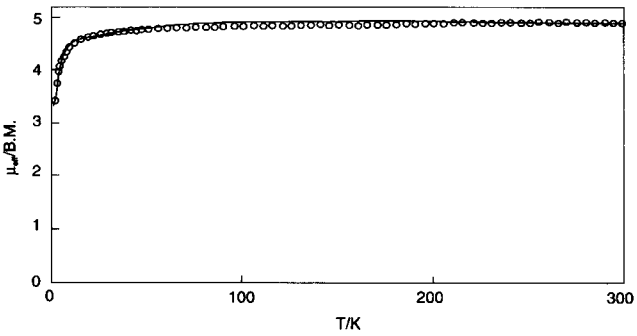

Fig. 6. Temperature dependence of magnetic moment per Ru(II,III)–(*p*-nitpy)$_2$ unit for **3**. The solid line is drawn with parameters listed in Table 4.

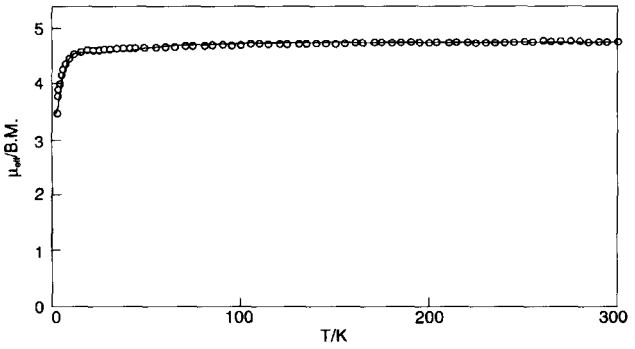

Fig. 7. Temperature dependence of magnetic moment per Ru(II,III)–(*p*-nitpy) unit for **4**. The solid line is drawn with parameters listed in Table 4.

within the Ru(II,III) dimeric core (e.g., D = 60 cm^{-1} for $[Ru_2(O_2CCMe_3)_4(H_2O)_2]BF_4$).[10,12b] Also, there is an important difference in the magnetic behavior below ca. 50 K between the *p*-nitpy and *m*-nitpy adducts. The decrease in the magnetic moments of **1** and **2** begins at ca. 50 K when the temperature is lowered, while the moments do not decrease until ca. 5 K for **3** and **4**. We thus analyzed the magnetic behavior of the adducts while considering this difference. The possible interactions in the present system are depicted in Scheme 1, where the intramolecular radical–radical interaction (J_{R-R}) are not taken into consideration, and are set at 0 cm^{-1} because the interaction through the coordinated pyridyl group is too weak (see below) to give the significant radical–radical interaction. A quantum treatment based on the spin Hamiltonian, however, is still too complicated to introduce all of the other magnetic interactions into the theoretical equation. Hence, we applied a molecular-field approximation[8] to the weaker interaction (J_{M-R} or $J_{R\cdots R}$) on the condition that one of the J values is considerably smaller than the other. In the case of $|J_{R\cdots R}| \ll |J_{M-R}|$, the intradimer interaction between the Ru(II,III) dimer and the radical is predominant, here being termed model A.[14] In the case of $|J_{M-R}| \ll |J_{R\cdots R}|$, the interaction between the nitroxide radicals of the neighboring cation units through the space is predominant, here being termed model B.[15,16] Because the interactions are both essentially weak compared to the zero-field splitting, we estimated the J values by fixing D = 50 cm^{-1}. This qualitative analysis was effective to explain the difference between the *m*-nitpy and *p*-nitpy adducts at temperatures below 50 K. As shown in Figs. 4 and 5, the cryomagnetic behaviors of **1** and **2**·0.5 CH_2Cl_2 were sufficiently simulated using an equation based on model A. An equation based on model B was not able to well reproduce the behavior at the low-temperature region (see the insets of Figs. 4 and 5). The obtained magnetic parameters are listed in Table 4, in which g_M and g_{nit} are the g factors of the Ru(II,III) core and the nitroxide ligand, respectively. The radical–radical interaction ($J_{R\cdots R}$) was estimated to be nearly zero based on a molecular-field approximation. On the contrary, the magnetic behaviors of **3** and **4** could be explained by model B, as shown in Figs. 6 and 7. The parameters used for the simulation are listed in Table 4. Interestingly, the J values for the Ru(II,III)–radical interaction obtained by a molecular field approximation are positive (0.8 cm^{-1} for **3** and 1.4 cm^{-1} for **4**), which is responsible for well reproducing the plateau at the low-temperature region. This result can be explained by the spin-polarization mechanism[8] through the pyridyl group by taking into account that the dihedral angle between the pyridine ring and the ONCNO plane of *m*-nitpy and *p*-nitpy is almost the same (ca. 30°) in **1** and **4**·0.5CH_2Cl_2. In the case of **3** and **4**, there is an odd number of the atoms between the paramagnetic Ru(II,III) core and the N–O group through the π-system between two N–O groups and that of the pyridyl group in *p*-nitpy, while, in the case of **1** and **2**·0.5CH_2Cl_2, an even number of atoms exist between the Ru(II,III) core and the N–O group of *m*-nitpy. The chain complex of the Ru(II,III) dimeric cation $[Ru_2(O_2CCMe_3)_4(p\text{-nitpy})]_n(BF_4)_n$ revealed a weak ferromagnetic interaction through the coordinated pyridyl group (J_{M-R} = 0.45 cm^{-1}) between the

Table 4. Fitting Parameters for the Magnetic Data

	1	**2**·0.5CH_2Cl_2	**3**	**4**
g_M	2.3	2.3	2.25	2.09
g_{nit}	2.0	2.0	2.0	2.0
D/cm^{-1}	50	50	50	50
J_{M-R}	−1.0	−1.0	0.8[a)]	1.4[a)]
J_{R-R}	0	0	0	0
$J_{R\cdots R}$	0	0	−5.0	−6.0
$R/10^3$ [b)]	18	26	1.8	5.8

a) Estimated by a molecular field approximation.
b) $R = \sum(\chi_{obsd} - \chi_{calcd})^2/\sum(\chi_{obsd})^2$, where χ is the magnetic susceptibility.

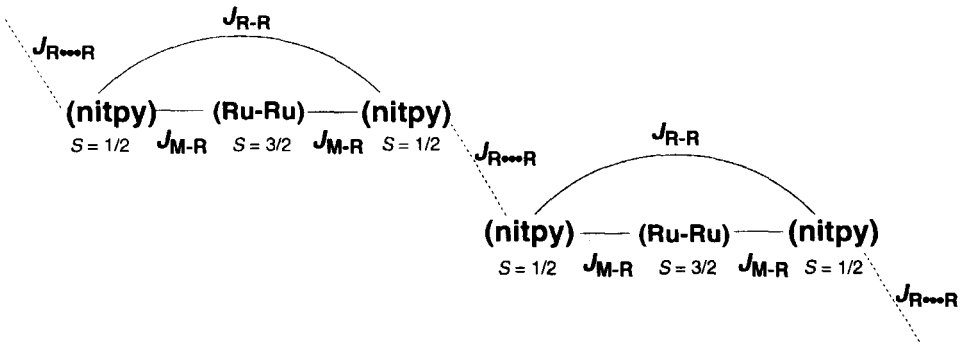

Scheme 1.

Ru(II,III) core and the radical.[5] The difference in magnitude of the through-space radical interaction ($J_{R\cdots R}$) between the *m*-nitpy adducts (0 cm^{-1} for **1** and **2**·0.5 CH_2Cl_2) and the *p*-nitpy ones (−5.0 cm^{-1} for **3** and −6.0 cm^{-1} for **4**) is now unclear. Although this could be related to the different way of contact between the uncoordinated nitroxide oxygen atoms (Fig. 3), the observed contact for **1** should give an antiferromagnetic interaction to some degree.[17] At present, we can not present any conclusive discussion on this problem, and need to collect more data on many adduct complexes of pyridyl nitronyl nitroxide radicals in combination with the ruthenium(II,III) carboxylate dimers.

In this study, we first successfully prepared bis-adduct complexes of the ruthenium(II,III) dimeric cation and the pyridyl nitronyl nitroxide radicals $[Ru_2(O_2CCMe_3)_4(L)_2]X$ (L = *m*-nitpy and *p*-nitpy; X = BF_4 and BPh_4). It has been crystallographically confirmed that the coordination of the pyridyl groups occurs at both the axial sites of the Ru(II,III) cation core by the X-ray diffraction method. Weak magnetic interactions between the radical and Ru(II,III) dimer through the pyridyl group and the radicals of the neighboring cation units through the space were observed. Our interest is now directed to the use of the bis-adduct units as building blocks by linkage of the uncoordinated N–O groups to the paramagnetic metal ions to produce highly dimensional magnetic materials. Such a study is under way in our laboratories.

The present work was partially supported by a Grant-in Aid for Scientific Research (No. 10640547) from the Ministry of Education, Science, Sports and Culture and by a grant from the Mitsubishi Chemical Corporation Fund.

References

1 a) A. Caneschi, D. Gatteschi, R. Sessoli, and P. Rey, *Acc. Chem. Res.*, **22**, 392 (1989). b) A. Caneschi and D. Gatteschi, *Prog. Inorg. Chem.*, **39**, 331 (1991).

2 M. Handa, Y. Sayama, M. Mikuriya, R. Nukada, I. Hiromitsu, and K. Kasuga, *Bull. Chem. Soc. Jpn.*, **71**, 119 (1998).

3 a) M. Handa, Y. Sayama, M. Mikuriya, R. Nukada, I. Hiromitsu, and K. Kasuga, *Bull. Chem. Soc. Jpn.*, **68**, 1647 (1995). b) M. Handa, Y. Sayama, M. Mikuriya, R. Nukada, I. Hiromitsu, and K. Kasuga, *Chem. Lett.*, **1996**, 201. c) Y. Sayama, M. Handa, M. Mikuriya, I. Hiromitsu, and K. Kasuga, *Chem. Lett.*, **1999**, 453.

4 a) A. Caneschi, F. Ferraro, D. Gatteschi, P. Rey, and R. Sessoli, *Inorg. Chem.*, **29**, 1756 (1990). b) A. Caneschi, F. Ferraro, D. Gatteschi, P. Rey, and R. Sessoli, *Inorg. Chem.*, **29**, 4217 (1990). c) A. Caneschi, F. Ferraro, D. Gatteschi, P. Rey, and R. Sessoli, *Inorg. Chem.*, **30**, 3162 (1991). d) A. Caneschi, D. Gatteschi, R. Sessoli, and P. Rey, *Inorg. Chim. Acta*, **184**, 67 (1991). e) C. Benelli, A. Caneschi , D. Gatteschi, and L. Pardi, *Inorg. Chem.*, **31**, 741 (1992). f) D. Luneau, G. Risoan, P. Rey, A. Grand, A. Caneschi, D. Gatteschi, and J. Laugier, *Inorg. Chem.*, **32**, 5616 (1993). g) F. L. de Panthou, E. Belorizky, R. Camlemczuk, D. Luneau, C. Marcenat, E. Ressouche, P. Turek, and P. Rey, *J. Am. Chem. Soc.*, **117**, 11247 (1995). h) K. Fegy, N. Sanz, D. Luneau, E. Belorizky, and P. Rey, *Inorg. Chem.*, **37**, 4518 (1998). i) C. -J. Lee, C. -H. Huang, H. -H. Wei, Y. -H. Liu, G. -H. Lee, and Y. Wang, *J. Chem. Soc., Dalton Trans.*, **1998**, 171. j) T. Yoshida and S. Kaizaki, *Inorg. Chem.*, **38**, 1054 (1999). k) T. Yoshida, T. Suzuki, K. Kanamori, and S. Kaizaki, *Inorg. Chem.*, **38**, 1059 (1999). l) M. Fettouhi, M. Khaled, A. Waheed, S. Golhen, L. Ouahab, J. -P. Sutter, and O. Kahn , *Inorg. Chem.*, **38**, 3967 (1999). m) Y. -H. Chung , H. -H. Wei, G. -H. Lee, Y. Wang, *Inorg. Chim. Acta*, **293**, 30 (1999). n) Y. -H. Chung and H. -H. Wei, *Inorg. Chem. Commun.*, **2**, 269 (1999). o) I. Dasna, S. Golhen, L. Ouahab, O. Pena, J. Guillevic, and M. Fettouhi, *J. Chem. Soc., Dalton Trans.*, **2000**, 129.

5 Y. Sayama, M. Handa, M. Mikuriya, I. Hiromitsu, and K. Kasuga, *Chem. Lett.*, **1998**, 777.

6 M. C. Barral, R. Jiménez-Aparicio, J. L. Priego, E. C. Royer, E. Gutiérrez-Puebla, and C. Ruiz-Valero, *Polyhedron*, **11**, 2209 (1992).

7 E. F. Ullman, L. Gall, and J. H. Osiecki, *J. Org. Chem.*, **35**, 3623 (1970); M. S. Davis, K. Morokuma, and R. W. Kreilick, *J. Am. Chem. Soc.*, **94**, 5588 (1972).

8 O. Kahn, "Molecular Magnetism," VCH Publishers Inc. (1993).

9 C. K. Fair, "MolEN Structure Determination System," Delft Instrument, Delft (1990).

10 Y. Sayama, M. Handa, M. Mikuriya, R. Nukada, I. Hiromitsu, and K. Kasuga, *Coordination Chemistry at the Turn of the Century*, **4**, 447 (1999).

11 K. Nakamoto, "Infrared and Raman Spectra of Inorganic and Coordination Compounds," 4th ed, Wiley Interscience, New York (1986).

12 a) F. A. Cotton and R. A. Walton, "Multipule Bonds between Metal Atoms," 2nd ed, Oxford Univ. Press, New York (1993). b) M. A. S. Aquino, *Coord. Chem. Rev.*, **170**, 141 (1998).

13 K. Awaga, T. Inabe, and Y. Maruyama, *Chem. Phys. Lett.*, **190**, 349 (1992).

14 The corresponding spin Hamiltonian and its quantum treatment can be seen in Ref. 3a.

15 B. Bleaney and K. D. Bowers, *Proc. R. Soc. London, Ser. A:*, **214**, 451 (1952); Bleaney–Bowers equation for the (S = 1/2)—(S = 1/2) system is applicable to the radical (S = 1/2)—radical (S = 1/2) interaction.

16 The system is schematically shown below.

$$\underset{S=1/2}{(\text{nitpy})}\overset{J_2}{\text{—}}\underset{S=1/2}{(\text{nitpy})}\overset{J_1}{\text{—}}\underset{S=3/2}{(\text{Ru}_2)}\overset{J_1}{\text{—}}\underset{S=1/2}{(\text{nitpy})}\overset{J_2}{\text{—}}\underset{S=1/2}{(\text{nitpy})}\overset{J_1}{\text{—}}\underset{S=3/2}{(\text{Ru}_2)}\overset{J_1}{\text{—}}$$

When the effect of J_1 is taken into account by a molecular-field approximation, a following equation is obtained.

$$\chi = \frac{\chi_1 + \chi_2 + 2A\chi_1\chi_2}{1 - A^2\chi_1\chi_2}$$

where

$$A = \frac{2J_1Z}{g_1g_2\mu_B^2N},\ Z = 2,\ \chi_1 = \frac{2Ng_1^2\mu_B^2}{kT}\frac{1}{3+e^{-2J_2/kT}},\ \text{and}$$

$$\chi_2 = \frac{Ng_2^2\mu_B^2}{kT}\left\{\frac{3}{4} + \frac{1}{2(D/kT)}\frac{1-e^{-2D/kT}}{1+e^{-2D/kT}}\right\},$$

χ_1 being the susceptibility for the radical pair and χ_2 for the Ru(II, III) core.

17 A. Cogne, A. Grand, P. Rey, and R. Subra, *J. Am. Chem. Soc.*, **111**, 3230 (1989); F. L. de Panthou, D. Luneau, J. Laugier, and P. Rey, *J. Am. Chem. Soc.*, **115**, 9095 (1993).